
Householder-Absolute Neural Layers For High Variability and Deep Trainability

Yueyao Yu and Yin Zhang

The Chinese University of Hong Kong, Shenzhen
Shenzhen, Guangdong, China

Abstract

We propose a new architecture for artificial neural networks called Householder-absolute neural layers, or Han-layers for short, that use Householder reflectors as weight matrices and the absolute-value function for activation. Han-layers, functioning as fully connected layers, are motivated by recent results on neural-network variability and are designed to increase activation ratio and reduce the chance of Collapse to Constants. Neural networks constructed chiefly from Han-layers are called HanNets. By construction, HanNets enjoy a theoretical guarantee that vanishing or exploding gradient never occurs. We conduct several proof-of-concept experiments. Some surprising results obtained on styled test problems suggest that, under certain conditions, HanNets exhibit an unusual ability to produce nearly perfect solutions unattainable by fully connected networks. Experiments on regression datasets show that HanNets can significantly reduce the number of model parameters while maintaining or improving the level of generalization accuracy. In addition, by adding a few Han-layers into the pre-classification FC-layer of a convolutional neural network, we are able to quickly improve a state-of-the-art result on CIFAR10 dataset. These proof-of-concept results are sufficient to necessitate further studies on HanNets to understand their capacities and limits, and to exploit their potentials in real-world applications.

1 Introduction

Deep neural networks (DNN) have greatly advanced the state of the arts in many machine learning tasks such as image classification, text categorization, speech recognition, to name just a few out of a long list. The most fundamental architectural component of DNNs are hidden layers of various kinds, including the most generic fully-connected (FC) layers and the highly successful convolutional layers [12] most widely used in computer vision. The primary objective of this work is to propose a new hidden-layer architecture along with a proof-of-concept evaluation on its merits.

Our work is motivated by recent results in [28] on variability of DNNs. Variability is a qualitative surrogate of expressivity (see [5] for a recent survey on expressivity) for DNNs, and is shown in [28] to be closely connected to deep trainability of fully connected neural nets with ReLU activations. To an extent, the higher variability is for a given model, the easier it is to train the model to reach high-quality solutions. It is shown in [28] that variability rises with a key quantity called *activation ratio* or AR (see (4) for definition), and falls with the occurrence of a phenomenon called Collapse to Constant (C2C), which is closely related to gradient vanishing but not identical. The results in [28] provide a useful new angle to view the efficacy of neural nets. Guided by the variability viewpoints,

we propose a novel neural-layer design aimed to increase activation ratio and decrease the chance of C2C at the same time.

1.1 Contributions

In this work, we propose a new architecture called Householder-absolute neural Network (HanNet) aimed to obtain higher variability with fewer parameters. As the name suggests, in a fully connected layer we replace the square weight matrix by a Householder reflector and use absolute-value function for activation.

1. By design, HanNet achieves a high activation ratio. The construction of it also guarantees that neither vanishing nor exploding gradient will ever occur. The chance of Collapse to Constants, yet not completely eliminated in theory, has also been greatly diminished.
2. Our proof-of-concept study indicates that HanNets, while reducing the number of parameters from fully connected models by orders of magnitude, HanNets can still maintain, and often improve, generalization performance. Potentially, this feature will have usefulness in deployments of deep learning models to, for example, mobile devices.
3. On styled model problems, we observe a stunning generalization power in HanNets. As is illustrated in Figure 1, a HanNet produces nearly perfect results on a synthetic, yet difficult dataset, outperforming fully connected networks (FCNets) by a huge margin in terms of test accuracy, despite both achieving nearly 100% training accuracy. More details will be reported in Section 3.2.1.

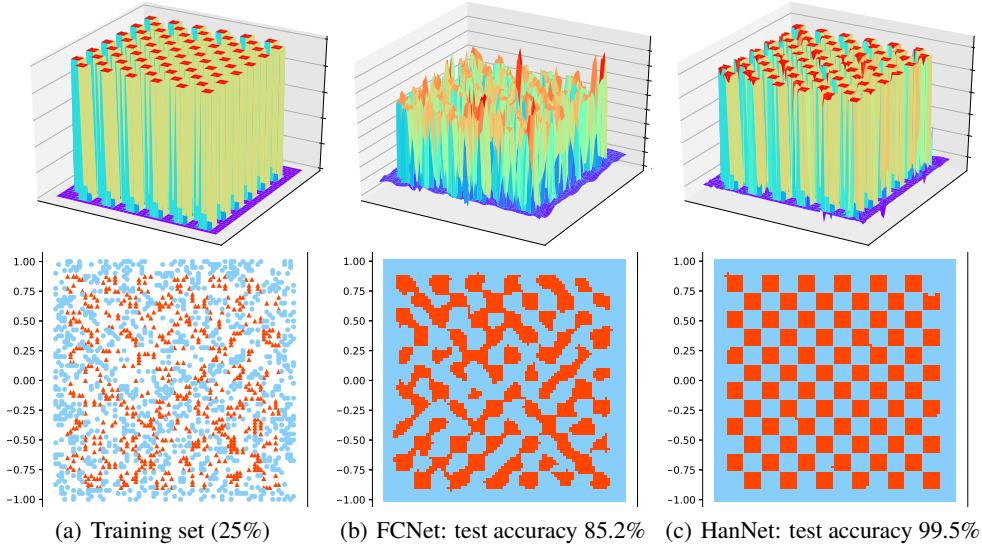


Figure 1: The top row consists 3 functions (from left to right): the target binary function, a function trained from a FCNet and one from a HanNet, respectively. The bottom row: (a) plots the training set with 25% of data points, (b) and (c) are top views of the two trained solutions (rounded to 0 or 1), along with their test accuracies. The training accuracies are nearly 100% for both.

Many important issues remain to be investigated in order to understand the powers and the limits of HanNets, and to unlock their potentials in real-world applications.

1.2 Related Works

As is mentioned, the two key building blocks in our proposed HanNets are (1) the absolute-value function (ABS) for activations, and (2) the Householder reflectors as weight matrices, which are orthogonal matrices.

In earlier periods of neural network research, piece-wise linear model structures were considered that involved ABS functions [3, 14]. However, over the last three decades, ABS has never entered the mainstream; in fact, it has rarely been utilized at all. It turns out that another piece-wise linear function ReLU [16] has gained popularity and become arguably the most widely used activation function nowadays. The author in [9] proposes to use the ABS activation in a “bidirectional neuron” (autoencoder-like) architecture based on an interpretability consideration. Recently, the authors in [28] show that, under the same conditions, ABS can better resist the occurrence of C2C and thus better maintain network variability than ReLU.

Orthogonal weight-matrix initializations have attracted theoretical and empirical investigations and found significant successes in deep learning, to cite a few see [7, 8, 13, 19, 26]. Restricting weight matrices to be orthogonal has also been utilized in the recurrent and convolution neural networks [15, 20, 22, 23, 25, 27]. The orthogonal RNN (oRNN) [15] uses products of Householder reflection matrices to represent transition matrices in an effort to alleviate the problems caused by vanishing or exploding gradient. The authors in [28] demonstrate that orthogonal initializations also help retain variability as network depth grows.

1.3 Notations

For a given activation function $\phi(\cdot)$ and a sequence of weight-bias (matrix-vector) pairs $\{(W_i, b_i)\}$ of proper sizes, we first define layer functions

$$\psi_i(\cdot) \equiv \psi_i(\cdot, W_i, b_i) := W_i \phi_i(\cdot) + b_i, \quad i = 1, 2, \dots, \quad (1)$$

which is the composition of an affine function, constructed from (W_i, b_i) , with the activation function $\phi_i(\cdot)$. As is done above, we will drop the dependence of ψ_i on the parameter pair (W_i, b_i) whenever no confusion arises. For any positive integer k ,

$$F_k(x) := (\psi_k \circ \dots \circ \psi_1)(x), \quad (2)$$

which is the composition of the functions ψ_1 up to ψ_k , parameterized by the weight-bias pairs (W_i, b_i) for $i = 1, \dots, k$. In general, $W_i \in \mathbb{R}^{n_{i+1} \times n_i}$, $b_i \in \mathbb{R}^{n_{i+1}}$ and $\phi_i : \mathbb{R}^{n_{i+1}} \rightarrow \mathbb{R}^{n_{i+1}}$, thus function $F_k(x)$ is from \mathbb{R}^{n_1} to \mathbb{R}^{n_k} . For an L -layer DNN, the model output is $F_L(x; \mathbf{W}, \mathbf{b})$, where $\mathbf{W} = \{W_1, \dots, W_L\}$ and $\mathbf{b} = \{b_1, \dots, b_L\}$.

1.4 Variability and Metrics

Qualitatively, variability represents the richness of landscape variations of neural networks over a relevant parameter region. A network with higher variability means it is more expressive in data space and at the same time more sensitive to parameter change in a relevant parameter region. Conversely, lower variability means that it is more likely for a DNN to have poor approximation and/or generalization abilities, and consequently may be more difficult to reach high-quality solutions. In particular, the worst case scenario is that a neural network loses all of its variability and, for parameters from certain region, becomes a constant in the entire or a part of date space. It is called C2C (collapse to constant) [28].

A measurement of variability used in [28] is

$$V := \mathbb{E}_{(\mathbf{W}, \mathbf{b})} \left(\|f\|^{-2} \int_{\Omega} \sum_{i=1}^n \left| \frac{\partial^3 f}{\partial^3 x_i} \right|^2 dx \right) \quad (3)$$

where $f \equiv f(F_L(x; \mathbf{W}, \mathbf{b}))$ is a scalar-valued loss function for an L -layer DNN $F_L(x; \mathbf{W}, \mathbf{b})$, Ω is a relevant region in the data space and $\mathbb{E}_{(\mathbf{W}, \mathbf{b})}$ is a sample mean over initialized parameter samples. We will use this quantity to compare levels of variability for different initialization strategies.

Evidently, the source of variability is the nonlinear activations applied to individual neurons in a DNN. A key quantity is called the activation ratio (AR) below, as defined in [28],

$$AR = \frac{\text{total number of individual activations}}{\text{total number of model parameters}}, \quad (4)$$

which is shown to be proportionate to network variability until the effects of C2C start to show up for deep networks [28]. In this work, we will also use AR as one of the metrics for variability. However, we caution against the simplistic view that the higher the AR or variability is, the better. In fact, experiments indicate that excessive nonlinearity tends to increase training difficulties .

2 HanNet: Fewer Parameters and Higher Variability

A path to enhancing and maintaining variability of a DNN is to raise its resistance level to C2C and increase its AR simultaneously. Our construction of Han-layers follows exactly this path.

2.1 ABS Activation: C2C-Resistive

It is reported in [28] that ABS is less prone to C2C (collapse to constants) than ReLU is. In Figure 2, we visualize variability for three networks: (i) FCNet with ReLU, (ii) FCNet with ABS, and (iii) (to be proposed) HanNet, which uses ABS. All three networks are of size 70×10 , i.e. having 70-hidden-layer with 10 neurons per layer, plus input and output layers. The input data are a set of grid points on the square $[-1, 1]^2$ and the output is two-dimensional as well. The plotted surface is the average values of the outputs. Each row of Figure 2 contains 4 plots for 4 normally distributed parameter samples scaled by standard initialization factors. We observe that C2C-effects are clearly present with ReLU activation, but barely observable with ABS. HanNet surely enjoys the best variability.

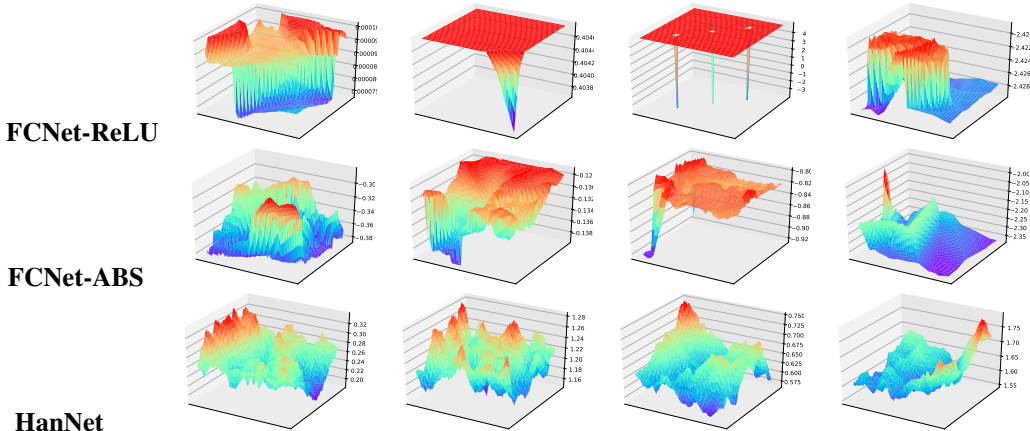


Figure 2: Visualization of variability on three DNNs with 70 hidden layers

We perform a test similar to what is in Section 3.2 of [28] to study the relationship between variability and trainability while fixing the number of model parameters at 3200 (the number of training samples is about 1600). Here, we compare FCNet-ReLU with FCNet-ABS. The dataset is an easier Checkerboard problem with 8 by 8 blocks rather than 12 by 12 as in Figure 1. We reports training and testing performances in Figure 3. We observe that on models with more than 20 hidden layers, FCNet-ReLU is unable to reach near-zero loss values, but FCNet-ABS still succeeds even after the hidden-layer number exceeds 30, confirming that ABS works better than ReLU in deeper DNNs.

2.2 Householder Weighting: Orthogonal and High AR

It is well-known that Householder reflection matrix associated with a nonzero vector $u \in \mathcal{R}^n$ is

$$H(u) = I - 2uu^\top/\|u\|^2, \quad (5)$$

which is symmetric and orthogonal. As is discussed earlier, orthogonality is a desirable property for weight matrices in DNNs. In addition, the degree of freedom in $H(u)$ is n , one order of magnitude smaller than $O(n^2)$ for a generic orthogonal matrix.

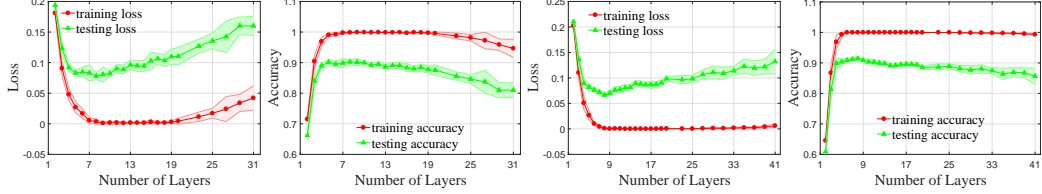


Figure 3: Training and testing performance of FCNets ReLU and ABS. The first two figures are for ReLU results, one for loss values and one for accuracies; and the last two figures are for ABS.

Obviously, one can increase the activation ratio of a DNN by reducing the number of model parameters without changing the network depth and width, such as by parametrizing an $n \times n$ weight matrix with far less than $O(n^2)$ parameters (similar to what is done in CNNs). This motivates us to use a Householder reflection matrix to replace a general or a generic orthogonal weight matrix in a neural layer so that the AR value associated with this layer is enlarged by a factor of $O(n)$.

In natural language processing areas, it has been proposed [15] to use a product of multiple Householder reflection matrices to parameterize a general weight matrix. This practice does not take the full advantage of the Householder weighting strategy from the viewpoint of enhancing variability.

2.3 Han-layers, HanNets and High Variability

A Householder-absolute neural layer, or Han-layer, is composed of a Householder matrix followed by ABS activation, as is given in Algorithm 1; and a HanNet is created by a sequence of Han-layers.

Algorithm 1 HanLayer.

Input: vector x and parameters (u, b) .
Output: $y = \text{HanLayer}(x; u, b)$

- 1: **function** HANLAYER(x, u, b)
- 2: $z = x - 2 \frac{u^T x}{\|u\|^2} u + b$ ▷ Householder Reflection plus bias
- 3: $y = \text{ABS}(z)$ ▷ Absolute-value Function Activation
- 4: **return** y
- 5: **end function**

Since pure Han-layers may not provide enough parameters, we sometimes need to add a few FC-layers to a HanNet architecture for the purpose of over-parameterization.

In Figure 2, we have already visualized the landscape of a deep HanNet, which has far more peaks and valleys than the others, indicating its higher variability. In Figure 4, we calculate the variability measure V defined in (3) to compare HanNets with FCNets, where the geometric mean is used which will vanish whenever C2C occurs. We observe that once the number of hidden layers reaches 27 or larger, C2C happens to FCNet-ReLU. For FC-ABS, variability rises and then gradually declines due to the effect of C2C, though a fully-developed C2C never happens in the tested range of depth (up to 45 hidden layers). The variability of HanNets, on the other hand, remains at a high level without degradation in the entire tested range.

2.4 Gradient Vanishing or Exploding No More

Let the neural network function $F_L(x, \mathbf{W}, \mathbf{b})$ be defined in (2). Its derivative with respect to the weight-bias pairs are computed by the chain-rule. In particular, its partial derivative with respect to b_1 is a representative case,

$$\frac{\partial}{\partial b_1} F_L(x, \mathbf{W}, \mathbf{b}) = \nabla \phi(h_1) W_2^T \nabla \phi(h_2) \cdots W_L^T \nabla \phi(h_L),$$

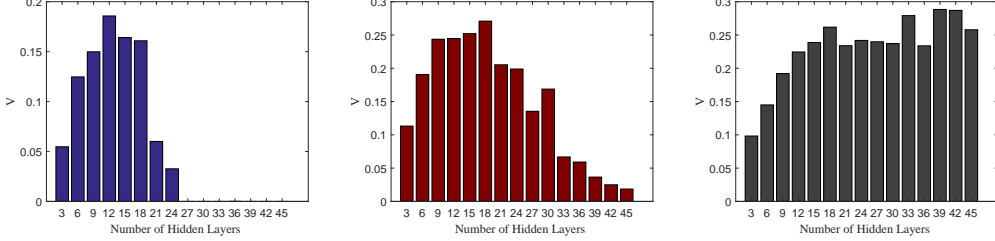


Figure 4: Computed variability measure in (3): left: FCNet-ReLU; middle: FCNet-ABS; right: HanNet. Each bar represents the *geometric mean* of 3000 samples of parameters. For FCNets, as the number of the hidden layers grows, the width decreases so that the total number of model parameters is approximately 4000. For HanNets, the fixed number of parameters is reduced from 4000 to 800.

where $h_k = F_k(x, \mathbf{W}, \mathbf{b})$, and $\nabla\phi(h_k)$ are diagonal matrices formed by applying scalar-valued ϕ to vectors component-wise. For ease of notation, we follow [28] and left-multiply W_1^T to the above matrix product (without loss of generality), and obtain the so-called G -matrix associated with the neural net function $F_L(x, \mathbf{W}, \mathbf{b})$,

$$G_L(x, \mathbf{W}, \mathbf{b}) := \prod_{k=1}^L W_k^T \nabla\phi(h_k). \quad (6)$$

The spectrum of this G -matrix characterizes whether vanishing or exploding gradient would happen or not. Specifically, as $L \rightarrow \infty$, vanishing gradient corresponds to $G_L \rightarrow 0$ and exploding gradient to $G_L \rightarrow \infty$. For HanNet, with the definition $\mathbf{u} = \{u_k\}_{k=1}^L$ we have

$$G_L(x, \mathbf{u}, \mathbf{b}) = \prod_{k=1}^L H(u_k) \nabla\phi(h_k), \quad (7)$$

where $H(u_k)$ is from (5), symmetric and orthogonal, and activation $\phi(t) = |t|$ which is not differentiable at $t = 0$. However, under any uniform distribution assumption, the probability for $t = 0$ is zero. Therefore, the diagonal matrices $\nabla\phi(h_k)$ are also orthogonal with diagonal entries equal to ± 1 . Since products of orthogonal matrices are orthogonal, by its very construction, HanNets will never suffer from either vanishing or exploding gradient. Evidently, the following result holds.

Proposition 1. *Under a uniform distribution assumption, the G -matrix for HanNet, that is, $G_L(x, \mathbf{u}, \mathbf{b})$ defined in 7, remains orthogonal with probability one for any x , any $u_i \neq 0$ in \mathbf{u} , any \mathbf{b} , and any integer $L > 0$.*

3 Proof-of-Concept Experiments

3.1 Datasets and Training

To empirically investigate the efficacy of HanNets in comparison to FCNets, we use the four datasets listed below in Table 1, including a synthetic dataset Checkerboard, 2 classic regression datasets, Elevators [4] and Cal Housing [17], and the widely used image classification dataset CIFAR-10 [11].

Our Checkerboard dataset is shown as Figure 1 with 6561 mesh points in a 12×12 block checkerboard over the square $[-1, 1]^2$. These mesh points are endowed with 0 or 1 labels according to their locations. We randomly pick 25% mesh points, about 1640, as our training set. We consider, and our experiments have confirmed, that this dataset is a highly challenging one for standard DNNs.

We use the mean-square error loss function for the checkerboard and the two regression datasets, and the cross-entropy loss function for CIFAR-10 to do image classification. We use stochastic gradient descent (SGD) with momentum to train Checkerboard and CIFAR-10. To solve each test instance,

Dataset	N	dim	Training percentage (%)
Checkerboard	6561	2	25
Elevators	16599	18	80 or 20
Cal Housing	20640	8	80 or 20
CIFAR-10	60000	2048	83.3

Table 1: Dataset statistics: N is the number of samples and dim the dimension of date vectors.

we run SGD using each of the following 10 initial learning rates:

$$\{0.001, 0.005, 0.01, 0.025, 0.05, 0.075, 0.1, 0.25, 0.5, 1\}$$

and select the best result as the output. In addition, the initial learning rate is annealed by a factor of 5 at the fractions 1/2, 7/10 and 9/10 of the training durations. Other parameter settings for SGD are listed in Table 2 below.

Dataset	Iteration	batch size	weight decay	momentum
Checkerboard	40000	100	0.0000	0.9
CIFAR-10	20000	1024	0.0001	0.9

Table 2: SGD parameters

For the two regression datasets, we choose Adam [10] as the training method which seems to be the method of choice for several works in that area including [21]. For Adam, the learning rate is set to 0.001 and the batch size is 100. The training duration is set to 300 epochs (epoch is used here for convenience of figure drawing).

All the training is done using PyTorch [18] running on a shared cluster. Finally, we mention that for each test instance, we always run 5 times starting from 5 different random initializations of model parameters. All the reported values are the average of 5 runs.

3.2 Results

3.2.1 Checkerboard

We compare three FCNets with a HanNet (in fact, more networks were compared, including ResNets, without better results than these three). Table 3 gives network statistics and test results for the involved 4 networks. We mention that in the HanNet, the first and the last hidden layers are fully connected for the reason of increasing the parameter number to a level of over-parameterization. Kaiming initialization [6] is used for FCNets, and orthogonal initialization for the two fully connected layers in the HanNet. In Section 1, we have already provided visualization (see Figure 1) of learned results from FCNet1 and HanNet, respectively, where the top views are generated by rounding computed function to 0 or 1.

Model	Depth \times Width	Param.	AR(%)	Train Acc(%)	Test Acc(%)
FCNet1	6×100	51002	1.17	99.97 ± 0.03	85.27 ± 0.35
FCNet2	10×100	91402	1.96	99.98 ± 0.02	85.34 ± 0.38
FCNet3	6×300	453002	0.39	100.0 ± 0.00	85.61 ± 0.17
HanNet	20×30	3032	19.78	99.98 ± 0.02	99.52 ± 0.27

Table 3: Testing accuracy on Checkerboard. HL denotes the number of hidden layers.

From Table 3, we observe that the training accuracies in all models are close to 100%, while in the term of the testing accuracy there is a large gap between the FCNets (around 85%) and HanNet (over

99%). The unexpected, near-perfect result, obtained by HanNet without any regularization, looks stunning, and is stable in the sense that similar results can be trained from other random 25%-75% data-splittings. However, such near-perfect solutions are not ubiquitous in the solution space.

To get a better grasp on how much the two HanNets components, Householder weighting and ABS activating, contribute to the surprising results on the Checkerboard dataset, we conduct an ablation study with four different configurations in a 20×30 network framework. The results are listed in Table 4 where the layer type is either Householder (H) or fully connected (FC) and the activation type is either ABS or ReLU. Table 4 suggests that Householder weighting and ABS activating be equally critical to the 99.5% generalization accuracy of the HanNet.

	Layer type		Activation type		Test accuracy
	H	FC	ABS	ReLU	
(a)	✓	✗	✓	✗	99.5%
(b)	✓	✗	✗	✓	76.8%
(c)	✗	✓	✓	✗	82.6%
(d)	✗	✓	✗	✓	82.3%

Table 4: Ablation study on a 20×30 network framework: Effects of layer and activation types on performance. H denotes Householder and FC denotes fully-connected layers.

To check the stability of the near-perfect result of the HanNet, we randomly flip 10% training labels as is shown in Figure 5 (a). The training result for FCNet1 is given in Figure 5 (b), while Figure 5 (c) and (d) are, respectively, the best and the last-iteration results for the HanNet in terms of testing accuracy. The best result shows that HanNet can still learn well the original pattern from seriously damaged labels. More curiously, the last-iteration result seems to suggest that, given enough time, HanNet can even learn more complex patterns with finer details than the original checkerboard pattern.

Our results on the Checkerboard dataset, as exciting as they are, seem to have posted more questions than answers. Are those hard-to-believe results purely accidental? Or the framework of HanNets does possess some unusual capacity under certain conditions? Further investigations are sorely needed to find out answers to these and other puzzling questions.

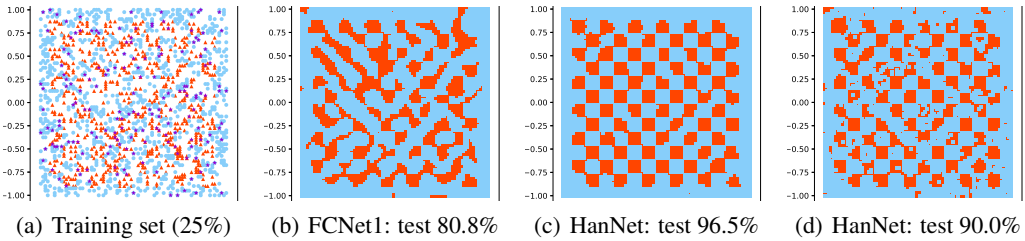


Figure 5: (a) Training set: violet-colored points are those whose labels are flipped (background color represents their original label). (b) FCNet1: the best testing and training accuracies are 80.8% and 94.3%, respectively. (c) HanNet: the best testing accuracy is 96.5% corresponding to 90.1% training accuracy. (d) HanNet: at the last iteration, training accuracy increases to 99.8% while testing accuracy decreases to around 90%. It appears that even accidentally created fine features have been faithfully learned by HanNet.

3.2.2 Regression Datasets

On the two regression Datasets, we compare the performance of a HanNet with two FCNets. Table 5 lists the relevant statistics for the 3 DNNs where depth refers to the number of hidden layers (there exist additional input/output layers). We see that in terms of parameter numbers FCNet1 and HanNet

are comparable peers, while FCNet2 has about 15 times more parameters. We mention that there is no FC layer in the HanNet beside the input and output layers.

Model	Depth \times Width	Elevators		Cal Housing	
		Parameters	AR(%)	Parameters	AR (%)
FCNet1	5×50	11201	2.23	10701	2.33
FCNet2	5×200	164801	0.60	162801	0.61
HanNet	20×200	11601	34.47	9601	41.66

Table 5: Model specifications and statistics of datasets (Elevators and Cal Housing)

We present testing NRMSE (normalized root mean square error) loss values in Figure 6, where the curves are average values over 5 trials with error bars.

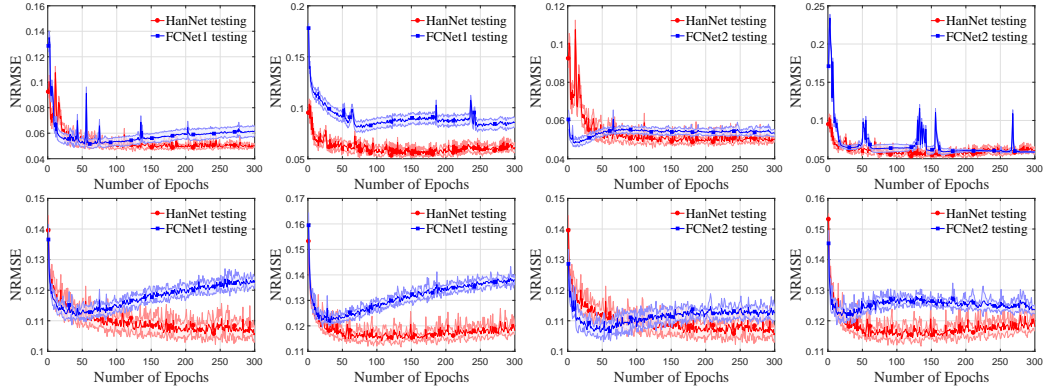


Figure 6: All figures show testing performance where the top row is for the Elevators dataset; and the bottom row for Cal Housing. From left to right: (1) HanNet (red) vs. FCNet1 (blue) on 80% training data, (2) then on 20% training data; (3) HanNet (red) vs FCNet2 (blue) on 80% training data, (4) then on 20% training data. Note that HanNet testing results are repeated.

Clearly, HanNet outperforms its “peer” FCNet1 by a notable margin, especially when fewer training samples are used, and is competitive with (on 80% training data) or better than (on 20% training data) FCNet2 which uses 15 times more parameters. We mention that the best testing performance of HanNet is statistically the same as that reported in [21] with a FCNet model that uses over 5 million parameters. Additionally, with fewer parameters HanNet appears less influenced by overfitting.

3.2.3 CIFAR-10

To explore the possibility for Han-layers to help improve state-of-the-art (SOTA) results, we extract feature vectors from the pre-trained CNN model LaNet [24] and carry out classification from that point on. According to the website [paperswithcode](#) [1], so far LaNet gives the best result (up to May 28, 2021) on CIFAR10 among all models not using extra training data (and 11th overall).

The feature vectors extracted from the LaNet model [2] are the input vectors of dimension 2048 into the last FC-layer before the final classification. We replace the 2048-to-10 FC-layer in LaNet with the following HanNet structure: a 2048-to-30 FC-layer, 3 Han-layers of width 30, and a 30-to-10 FC-layer. The result from training this HanNet structure is given in Table 6. We are able to slightly improve the top-1 testing error with a drop of about 10%. This result is stable as is shown by the relatively small standard deviation in 5 trials. We note that the LaNet result in Table 6 is taken directly from [2] as an average value.

	LaNet	with Han-layers
Top1 err(%)	0.99 ± 0.02	0.89 ± 0.02

Table 6: Top-1 testing error on CIFAR-10.

Such a quick improvement to the SOTA is encouraging, but far from a commonplace. Most times, SOTA models in image classification either use some complicating tricks such as extra training data or on-the-fly data augmentations, or allow no easy access to proper feature vectors (let alone that in many cases working codes are not publicly available).

4 Discussion

Built on the simple idea of increasing and maintaining variability, we propose the Han-layer architecture consisting of Householder weighting plus absolute-value activating. The former greatly raises activation ratio and at the same time keeps orthogonality, and the latter does its part in keeping its (diagonal) Jacobian orthogonal. Together, the combination of these two strategies provides the long-sought guarantee of eliminating both vanishing and exploding gradients from ever happening to deep HanNets. As defined, Han-layers can be used in place of fully-connected layers with an equal number of inputs and outputs, though the Han-layer construct can be easily extended to build more general DNN structures. For example, various extensions can be constructed to allow input data to be matrices and tensors, though their usefulness remains to be carefully studied.

We have conducted proof-of-concept experiments to evaluate the performance of HanNets against baseline performances provided by fully-connected networks. We make the following three remarks based on our current results.

1. We consider that our preliminary results are enough to support the claim that, in suitable situations, HanNets have the ability to significantly reduce the number of parameters and the associated computing costs, while maintaining or improving the level of generalization performance. Being much light-footed resource-wise, HanNet-based models are more likely to find deployment opportunities on low-power devices such as mobile phones.
2. HanNet structures can be added to existing models to improve their performance, even the state-of-the-art one, under suitable conditions. It is important to identify and understand such conditions in future investigations.
3. Under certain yet unclear conditions, HanNets appear to possess an unusual level of generalization ability, as is being demonstrated on the Checkerboard dataset. In our view, these results are too stable to be dismissed off-hand as being accidental. On the other hand, the possession of such an ability in general remains to be firmly established through theoretical studies and experiments on large-scale models. We plan to integrate Han-layer structures into more complex DNNs to help solve real-world application problems such as those in natural language processing.

References

- [1] <https://paperswithcode.com/sota/image-classification-on-cifar-10>.
- [2] <https://github.com/facebookresearch/LaMCTS/tree/master/LaNAS/LaNet>.
- [3] Roy Batrani. A multilayer neural network with piecewise-linear structure and back-propagation learning. *IEEE Transactions on Neural Networks*, 2(3):395–403, 1991.
- [4] Dheeru Dua and Casey Graff. UCI machine learning repository, 2017.
- [5] Ingo Gühring, Mones Raslan, and Gitta Kutyniok. Expressivity of deep neural networks. *arXiv preprint arXiv:2007.04759*, 2020.
- [6] Kaiming He, Xiangyu Zhang, Shaoqing Ren, and Jian Sun. Delving deep into rectifiers: Surpassing human-level performance on imagenet classification. In *Proceedings of the IEEE international conference on computer vision*, pages 1026–1034, 2015.
- [7] Wei Hu, Lechao Xiao, and Jeffrey Pennington. Provable benefit of orthogonal initialization in optimizing deep linear networks. In *International Conference on Learning Representations*, 2020.

- [8] Lei Huang, Xianglong Liu, Bo Lang, Adams Yu, Yongliang Wang, and Bo Li. Orthogonal weight normalization: Solution to optimization over multiple dependent stiefel manifolds in deep neural networks. In *Proceedings of the AAAI Conference on Artificial Intelligence*, volume 32, 2018.
- [9] Animesh Karnewar. Aann: Absolute artificial neural network. In *2018 3rd International Conference for Convergence in Technology (I2CT)*, pages 1–6. IEEE, 2018.
- [10] Diederik P Kingma and Jimmy Ba. Adam: A method for stochastic optimization. In *ICLR (Poster)*, 2015.
- [11] Alex Krizhevsky, Geoffrey Hinton, et al. Learning multiple layers of features from tiny images. Technical report, University of Toronto, 2009.
- [12] Alex Krizhevsky, Ilya Sutskever, and Geoffrey E Hinton. Imagenet classification with deep convolutional neural networks. *Advances in neural information processing systems*, 25:1097–1105, 2012.
- [13] Quoc V Le, Navdeep Jaitly, and Geoffrey E Hinton. A simple way to initialize recurrent networks of rectified linear units. *arXiv preprint arXiv:1504.00941*, 2015.
- [14] J-N Lin and Rolf Unbehauen. Canonical piecewise-linear approximations. *IEEE Transactions on Circuits and Systems I: Fundamental Theory and Applications*, 39(8):697–699, 1992.
- [15] Zakaria Mhammedi, Andrew Hellicar, Ashfaqur Rahman, and James Bailey. Efficient orthogonal parametrisation of recurrent neural networks using householder reflections. In *International Conference on Machine Learning*, pages 2401–2409. PMLR, 2017.
- [16] Vinod Nair and Geoffrey E Hinton. Rectified linear units improve restricted boltzmann machines. In *Icml*, 2010.
- [17] R Kelley Pace and Ronald Barry. Sparse spatial autoregressions. *Statistics & Probability Letters*, 33(3):291–297, 1997.
- [18] Adam Paszke, Sam Gross, Francisco Massa, Adam Lerer, James Bradbury, Gregory Chanan, Trevor Killeen, Zeming Lin, Natalia Gimelshein, Luca Antiga, et al. Pytorch: An imperative style, high-performance deep learning library. *Advances in Neural Information Processing Systems*, 32:8026–8037, 2019.
- [19] Jeffrey Pennington, Samuel Schoenholz, and Surya Ganguli. The emergence of spectral universality in deep networks. In *International Conference on Artificial Intelligence and Statistics*, pages 1924–1932. PMLR, 2018.
- [20] Jakub M Tomczak and Max Welling. Improving variational auto-encoders using householder flow. *arXiv preprint arXiv:1611.09630*, 2016.
- [21] Michael Tsang, Hanpeng Liu, Sanjay Purushotham, Pavankumar Murali, and Yan Liu. Neural interaction transparency (nit): Disentangling learned interactions for improved interpretability. In *NeurIPS*, pages 5809–5818, 2018.
- [22] Eugene Vorontsov, Chiheb Trabelsi, Samuel Kadoury, and Chris Pal. On orthogonality and learning recurrent networks with long term dependencies. In *International Conference on Machine Learning*, pages 3570–3578. PMLR, 2017.
- [23] Jiayun Wang, Yubei Chen, Rudrasis Chakraborty, and Stella X Yu. Orthogonal convolutional neural networks. In *Proceedings of the IEEE/CVF Conference on Computer Vision and Pattern Recognition*, pages 11505–11515, 2020.
- [24] Linnan Wang, Saining Xie, Teng Li, Rodrigo Fonseca, and Yuandong Tian. Sample-efficient neural architecture search by learning actions for monte carlo tree search. *IEEE Transactions on Pattern Analysis and Machine Intelligence*, 2021.
- [25] Scott Wisdom, Thomas Powers, John R Hershey, Jonathan Le Roux, and Les E Atlas. Full-capacity unitary recurrent neural networks. In *NIPS*, 2016.

- [26] Lechao Xiao, Yasaman Bahri, Jascha Sohl-Dickstein, Samuel Schoenholz, and Jeffrey Pennington. Dynamical isometry and a mean field theory of cnns: How to train 10,000-layer vanilla convolutional neural networks. In *International Conference on Machine Learning*, pages 5393–5402. PMLR, 2018.
- [27] Jiong Zhang, Qi Lei, and Inderjit Dhillon. Stabilizing gradients for deep neural networks via efficient svd parameterization. In *International Conference on Machine Learning*, pages 5806–5814. PMLR, 2018.
- [28] Yin Zhang and Yueyao Yu. Variability of artificial neural networks. arXiv 2105.08911, 2021.